

¹ Functional MRI brain state ² occupancy in the presence of ³ cerebral small vessel disease – a ⁴ pre-registered replication analysis of ⁵ the Hamburg City Health Study

✉ For correspondence:

e.schlemm@uke.de

Present address:

Dr. Dr. Eckhard Schlemm,
Klinik und Poliklinik für
Neurologie,
Universitätsklinikum
Hamburg-Eppendorf,
Martinistr. 52,
D-20251 Hamburg

Data availability:

Preprocessed data will be
available e.g. on
<https://github.com/csi-hamburg/HCHS-brain-states-RR>.

Funding: Deutsche
Forschungsgemeinschaft
(DFG) – SFB 936,
178316478 – C2 (Drs
Thomalla & Cheng)

Competing interests: The
authors declare no
competing interests.

⁶ Thies Ingwersen, MD  ¹, Carola Mayer, PhD ¹, Marvin Petersen, MD ¹,
⁷ Benedikt M. Frey, MD ¹, Jens Fiehler, MD ², Uta Hanning, MD ²,
⁸ Simone Kühn, PhD ^{3,4}, Jürgen Gallinat, MD ³, Raphael Twerenbold,
⁹ MD ⁵, Christian Gerloff, MD ⁶, Bastian Cheng, MD  ¹, Götz Thomalla,
¹⁰ MD ¹, Eckhard Schlemm, MBBS PhD  ¹✉

¹¹ Department of Neurology, University Medical Center

¹² Hamburg-Eppendorf; ²Department of Neuroradiology, University

¹³ Medical Center Hamburg-Eppendorf; ³Department of Psychiatry,

¹⁴ University Medical Center Hamburg-Eppendorf; ⁴Max-Planck-Institut für

¹⁵ Bildungsforschung, Berlin; ⁵Department of Cardiology, University

¹⁶ Medical Center Hamburg-Eppendorf; ⁶University Medical Center

¹⁷ Hamburg-Eppendorf

¹⁸ _____

¹⁹ Abstract

²⁰ **Objective:** To replicate recent findings  the association between the extent of
²¹ cerebral small vessel disease (cSVD), functional brain network dedifferentiation, and
²² cognitive impairment.

²³ **Methods:** We   demographic, imaging, and behavioral data from

24 the prospective population-based Hamburg City Health Study. Using a fully prespecified
25 analysis pipeline, we ~~will estimate~~ estimated discrete brain states from structural and
26 resting-state functional magnetic resonance imaging (MRI). In a multiverse analysis ~~we~~
27 ~~will vary~~, we varied brain parcellations and functional MRI confound regression
28 strategies. ~~Severity of cSVD will be operationalised~~ The severity of cSVD was
29 operationalized as the volume of white matter hyperintensities of presumed vascular
30 origin. Processing speed and executive dysfunction ~~are quantified by the trail making~~
31 ~~test~~ were quantified using the Trail Making Test (TMT).

32 **Hypotheses:** We ~~hypothesize~~ hypothesized a) that a greater volume of supratentorial
33 white matter hyperintensities ~~is~~ would be associated with less time spent in functional
34 MRI-derived brain states of high fractional occupancy; and b) that less time spent in
35 these high-occupancy brain states is associated with a longer time to completion in part
36 B of the TMT.

37 **Results:** High-occupancy brain states were characterized by activation or suppression
38 of the default mode network. Every 5.1-fold increase in WMH volume was associated
39 with a 0.94-fold reduction in the odds of occupying DMN-related brain states (P
40 5.01×10^{-8}). Every 5% increase in time spent in high-occupancy brain states was
41 associated with a 0.98-fold reduction in the TMT-B completion time ($P = 0.0116$). Findings
42 were robust across most brain parcellations and confound regression strategies.

43 **Conclusion:** We successfully replicated previous findings on the association between
44 cSVD, functional brain occupancy, and cognition in an independent sample. The data
45 provide further evidence for a functional network dedifferentiation hypothesis of
46 cSVD-related cognitive impairment. Further research is required to elucidate the
47 mechanisms underlying these associations.

48

49 Introduction

50 Cerebral small vessel disease (cSVD) is an arteriolopathy of the brain, ~~associated with age~~
51 and common cardiovascular risk factors (Wardlaw, C. Smith, and Dichgans, 2013). cSVD
52 predisposes ~~to ischemic~~, patients to ischemic stroke (in particular lacunar, ~~stroke~~stroke)
53 and may lead to cognitive impairment and dementia (Cannistraro et al., 2019). Neu-
54 roimaging findings in cSVD reflect its underlying pathology (Wardlaw, Valdés Hernández,
55 and Muñoz-Maniega, 2015) and include white matter hyperintensities (WMH) ~~and~~ la-

56 cunes of presumed vascular origin, small subcortical infarcts and microbleeds, enlarged
57 perivascular spaces as well as brain atrophy (Wardlaw, E. E. Smith, et al., 2013). However,
58 the extent of visible cSVD features on magnetic resonance imaging (MRI) is an imperfect
59 predictor of the severity of clinical sequelae (Das et al., 2019),⁷ and our understanding of
60 the causal mechanisms linking cSVD-associated brain damage to clinical deficits remains
61 limited (Bos et al., 2018).

62 Recent efforts have ~~concentrated~~focused on exploiting network aspects of the struc-
63 tural (Tuladhar, Dijk, et al., 2016; Tuladhar, Tay, et al., 2020; Lawrence, Zeestraten, et al.,
64 2018) and functional (Dey et al., 2016; Schulz et al., 2021) organization of the brain to
65 understand the ~~relation~~relationship between cSVD and clinical deficits in cognition and
66 other domains ~~reliant~~that rely on distributed processing. Reduced structural network ef-
67 ficiency has repeatedly been described as a causal factor in the development of cognitive
68 impairment, ~~in particular executive dysfunction and particularly executive dysfunction~~
69 and reduced processing speed,⁷ in cSVD (Lawrence, Chung, et al., 2014; Shen et al., 2020;
70 Reijmer et al., 2016; Prins et al., 2005). Findings with respect to functional connectivity
71 (FC), ~~on the other hand~~however, are more heterogeneous than their SC counterparts,
72 perhaps because FC measurements are prone to be affected by hemodynamic factors
73 and noise, resulting in relatively low reliability, especially with resting-state scans of short
74 duration (Laumann, Gordon, et al., 2015). This problem is exacerbated in the presence
75 of cSVD and ~~made worse by the~~worsened by arbitrary processing choices (Lawrence,
76 Tozer, et al., 2018; Gesierich et al., 2020).

77 As a promising new avenue, time-varying, or dynamic, functional connectivity approaches
78 have ~~more~~ recently been explored in patients with subcortical ischemic vascular disease
79 (Yin et al., 2022; Xu et al., 2021). ~~While~~Although the study of dynamic FC measures may
80 not solve the problem of limited reliability, especially in small populations or subjects
81 with extensive structural brain changes, it adds another – temporal – dimension to the
82 study of functional brain ~~organisation~~organization, which is otherwise overlooked. Im-
83 portantly, FC dynamics ~~do~~ not only reflect moment-to-moment fluctuations in cognitive
84 ~~processes~~processes, but are also related to brain plasticity and homeostasis (Laumann
85 and Snyder, 2021; Laumann, Snyder, et al., 2017), which may be impaired in cSVD.

86 In the present paper, we ~~aim~~aimed to replicate and extend the main results of (Schlemm
87 et al., 2022);⁸ In this recent study, the authors analyzed MR imaging and clinical data
88 from the prospective Hamburg City Health Study (HCHS, (Jagodzinski et al., 2020)) using

89 a coactivation pattern approach to define discrete brain states and found associations
90 between the WMH load, time spent in high-occupancy brain states characterized by ac-
91 tivation or suppression of the default mode network (DMN) ~~and cognitive impairment~~.
92 and cognitive impairment. Specifically, every 4.7-fold increase in WMH volume was
93 associated with a 0.95-fold reduction in the odds of occupying a DMN-related brain state;
94 every 2.5 seconds (i.e., one repetition time) not spent in one of those states was associated
95 with a 1.06-fold increase in TMT-B completion times.

96 The fractional occupancy of a functional MRI-derived discrete brain state is a subject-
97 specific measure of brain dynamics ~~and is~~ defined as the proportion of BOLD volumes
98 assigned to that state relative to all BOLD volumes ~~aquired~~acquired during a resting-
99 state scan.

100 Our primary hypothesis ~~is for the present work was~~ that the volume of supratentorial
101 white matter hyperintensities is associated with ~~the~~ fractional occupancy of DMN-related
102 brain states in a middle-aged to elderly population mildly affected by cSVD. Our ~~second~~
103 ~~hypothesis is that this secondary hypothesis was that~~ fractional occupancy is associated
104 with executive dysfunction and reduced processing speed, measured as the time to com-
105 plete part B of the ~~trail making test~~Trail Making Test (TMT).

106 Both hypotheses ~~will be~~were tested in an independent subsample of the HCHS study
107 population using the same imaging protocols, examination procedures, and analysis
108 pipelines as those in (Schlemm et al., 2022). The robustness of ~~associations will be explored~~
109 in the associations was explored using a multiverse approach by varying key steps in the
110 analysis pipeline.

111 Methods

112 Study population

113 ~~The paper will analyze~~This study analyzed data from the Hamburg City Health Study
114 (HCHS), ~~which is~~ an ongoing prospective, population-based cohort study aiming to re-
115 cruit a cross-sectional sample of 45 000 adult participants from the city of Hamburg, Ger-
116 many (Jagodzinski et al., 2020). From the first 10 000 participants of the HCHS ~~we will aim~~
117 , we planned to include those who were documented to have received brain imaging
118 ($n=2652$ ~~2648~~) and exclude those who were analyzed in our previous report (Schlemm et
119 al., 2022) ($n=970$). The ethical review board of the Landesärztekammer Hamburg (State
120 of Hamburg Chamber of Medical Practitioners) approved the HCHS (PV5131), ~~and~~ all par-

¹²¹ ticipants provided written informed consent.

¹²² Demographic and clinical characterization

¹²³ From the study database ~~we will extract~~, we extracted the participants' age at the time
¹²⁴ of inclusion in years, their ~~self-reported gender~~ sex, and the number of years spent
¹²⁵ in education. During the visit ~~at to~~ the study center, participants ~~undergo~~ underwent
¹²⁶ cognitive assessment using standardized tests. ~~We will extract from the database~~ From
¹²⁷ the database, we extracted their performance scores ~~in on~~ on the Trail Making Test part
¹²⁸ B, measured in seconds, as an operationalization of executive function and psychomo-
¹²⁹ tor processing speed (Tombaugh, 2004; Arbuthnott and Frank, 2000). For descriptive
¹³⁰ purposes, we also extracted data on past medical history and reported the proportion
¹³¹ of participants with a previous diagnosis of dementia.

¹³² MRI acquisition and preprocessing

¹³³ The magnetic resonance imaging protocol for the HCHS includes structural and resting-
¹³⁴ state functional sequences. The acquisition parameters ~~on for~~ a 3 T Siemens Skyra MRI
¹³⁵ scanner (Siemens, Erlangen, Germany) have been ~~reported before~~ previously reported
¹³⁶ (Petersen et al., 2020; Frey et al., 2021) and are given as follows:

¹³⁷ For T_1 -weighted anatomical images, a 3D rapid acquisition gradient-echo sequence
¹³⁸ (MPRAGE) was used with the following sequence parameters: repetition time TR = 2500 ms,
¹³⁹ echo time TE = 2.12 ms, 256 axial slices, slice thickness ST = 0.94 mm, and in-plane resolu-
¹⁴⁰ tion IPR = $(0.83 \times 0.83) \text{ mm}^2$.

¹⁴¹ T_2 -weighted fluid attenuated inversion recovery (FLAIR) images were acquired with
¹⁴² the following sequence parameters: TR = 4700 ms, TE = 392 ms, 192 axial slices, ST =
¹⁴³ 0.9 mm, IPR = $(0.75 \times 0.75) \text{ mm}^2$.

¹⁴⁴ 125 resting state functional MRI volumes were acquired (TR = 2500 ms; TE = 25 ms;
¹⁴⁵ flip angle = 90°; slices = 49; ST = 3 mm; slice gap = 0 mm; IPR = $(2.66 \times 2.66) \text{ mm}^2$). Subjects
¹⁴⁶ The subjects were asked to keep their eyes open and to think of nothing.

¹⁴⁷ We ~~will verify~~ verified the presence and ~~voxel-dimensions~~ voxel dimensions of ex-
¹⁴⁸ pected MRI data for each participant and ~~exclude~~ excluded those for whom at least
¹⁴⁹ one of T_1 -weighted, FLAIR, and resting-state MRI ~~is was~~ missing. We ~~will also exclude~~
¹⁵⁰ participants with a ~~also excluded participants with~~ neuroradiologically confirmed space-
¹⁵¹ occupying intra-axial lesion. To ensure reproducibility, no visual quality assessment ~~on~~
¹⁵² ~~raw images will be of raw images was~~ performed.

¹⁵³ For the remaining participants, structural and resting-state functional MRI data ~~will~~
¹⁵⁴ ~~be~~was preprocessed using FreeSurfer v6.0 (<https://surfer.nmr.mgh.harvard.edu/>), and fm-
¹⁵⁵ riPrep v20.2.6 (Esteban et al., 2019), using default parameters. Participants ~~will be~~were
¹⁵⁶ excluded if automated processing using at least one of these packages ~~fails~~failed.

¹⁵⁷ Quantification of WMH load

¹⁵⁸ For our primary analysis, the extent of ischemic white matter disease ~~will be~~was oper-
¹⁵⁹ ationalized as the total volume of supratentorial WMHs obtained from automated seg-
¹⁶⁰ mentation using a combination of anatomical priors, BIANCA (Griffanti, Zamboni, et al.,
¹⁶¹ 2016), and LOCATE (Sundaresan et al., 2019), post-processed with a minimum cluster
¹⁶² size of 30 voxels, as described in (Schlemm et al., 2022). In an exploratory analysis, we
¹⁶³ ~~partition~~partitioned voxels identified as WMH into deep and periventricular components
¹⁶⁴ according to their distance to the ventricular system (cut-off 10 mm, (Griffanti, Jenkinson,
¹⁶⁵ et al., 2018))

¹⁶⁶ Brain state estimation

¹⁶⁷ ~~Output from fMRIprep will be~~The output from fMRIprep was post-processed using xcpEngine
¹⁶⁸ v1.2.1 to obtain de-confounded spatially averaged BOLD time series (Ciric, Wolf, et al.,
¹⁶⁹ 2017). For the primary analysis~~we will use~~we used the 36p regression strategy and the
¹⁷⁰ Schaefer-400 parcellation (Schaefer et al., 2018), as in (Schlemm et al., 2022).

¹⁷¹ Different atlases and confound regression strategies, as implemented in xcpEngine,
¹⁷² ~~will be included in the~~were included in an exploratory multiverse analysis.

¹⁷³ Co-activation pattern (CAP) analysis ~~will be~~was performed by first aggregating parcel-
¹⁷⁴ lated, de-confounded BOLD signals into a ($n_{\text{parcels}} \times \sum_i n_{\text{time points},i}$) feature matrix, where
¹⁷⁵ $n_{\text{time points},i}$ denotes the number of retained volumes for subject i after confound re-
¹⁷⁶ gression. Clustering ~~will be~~was performed using the k -means algorithm ($k = 5$) with
¹⁷⁷ ~~a~~a distance measure given by 1 minus the sample Pearson correlation between points,
¹⁷⁸ as implemented in Matlab R2021a. We ~~will estimate~~estimated the subject- and state-
¹⁷⁹ specific fractional occupancies, which are defined as the proportion of BOLD volumes
¹⁸⁰ assigned to each brain state (Vidaurre et al., 2018). The two states with the highest aver-
¹⁸¹ age ~~occupancy~~occupancies ~~were~~were identified as the basis for further analysis.

182 **Statistical analysis**

183 For demographic (age, ~~gender, sex, and~~ years of education) and clinical (TMT-B) variables,
184 the number of missing ~~records will be items is~~ reported. For non-missing values, we
185 ~~will~~ provide descriptive summary statistics using median and interquartile range. The
186 ~~proportion proportions~~ of men and women in the sample ~~will be reported. Regression~~
187 ~~modelling will be are reported. Since we expected based on our pilot data~~ (Schlemm et al.,
188 2022) ~~that the proportion of missing data would be small, primary regression modelling~~
189 ~~was~~ carried out as a complete-case analysis.

190 As ~~a first an~~ outcome-neutral quality check of the implementation of the MRI process-
191 ing pipeline, brain state estimation, and co-activation pattern analysis, we ~~will compare~~
192 ~~compared~~ fractional occupancies between brain states. We ~~expect expected~~ that the av-
193 erage fractional occupancy in ~~the~~ two high-occupancy states ~~is would be~~ higher than the
194 average fractional occupancy in the other three states. Point estimates and 95% confi-
195 dence intervals ~~will be are~~ presented for the difference in average fractional occupancy
196 to ~~check verify~~ this assertion.

197 For further analyses, non-zero WMH volumes ~~will be subjected to a were subjected~~
198 ~~to~~ logarithmic transformation. Zero values ~~will retain their value retained their value of~~
199 zero; to compensate, all models ~~will include included~~ a binary indicator for zero WMH
200 volume if at least one non-zero ~~value is WMH value was~~ present.

201 To assess the primary hypothesis of a negative association between the extent of
202 ischemic white matter disease and time spent in high-occupancy brain states, we ~~will~~
203 ~~perform performed~~ a fixed-dispersion ~~beta-regression Beta regression~~ to model the logit
204 of the conditional expectation of the average fractional occupancy of two high-occupancy
205 states as an affine function of the logarithmized WMH load. Age and ~~gender will be sex~~
206 ~~were~~ included as covariates. The strength of the association ~~will be quantified as an was~~
207 ~~quantified as the~~ odds ratio per interquartile ratio of the WMH burden distribution ~~and~~
208 ~~and is~~ accompanied by a 95% confidence interval. Significance testing of the null hy-
209 pothesis of no association ~~will be was~~ conducted at the conventional significance level of
210 0.05. Estimation and testing ~~will be were~~ carried out using the 'betareg' package v3.1.4
211 in R v4.2.1.

212 To assess the secondary hypothesis of an association between time spent in high-
213 occupancy brain states and executive dysfunction, we ~~will perform performed~~ a general-
214 ized linear regression with a Gamma response distribution to model the logarithm of the

215 conditional expected completion time in part B of the TMT as an affine function of the
216 average fractional occupancy of two high-occupancy states. Age, ~~gender~~sex, years of ed-
217 ucation, and logarithmized WMH load ~~will be~~were included as covariates. The strength of
218 the association ~~will be~~was quantified as a multiplicative factor per percentage point and
219 accompanied by a 95% confidence interval. Significance testing of the null hypothesis of
220 no association ~~will be~~was conducted at the conventional significance level of 0.05. Esti-
221 mation and testing ~~will be carried out~~were performed using the `glm` function included
222 in the 'stats' package from R v4.2.1.

223 ~~Sample size calculation is~~

224 Pre-registered analyses

225 The analysis plan was pre-registered on June 27 2023 at <https://osf.io/fcqmb>. The sample
226 size calculation was based on an effect size on the odds ratio scale of 0.95, correspond-
227 ing to an absolute difference in the probability of occupying a DMN-related brain state
228 between the first and third WMH-load quartile of 1.3 percentage points, and between
229 the 5% and 95% percentile of 3.1 percentage points. Approximating half the difference
230 in fractional occupancy of DMN-related states between different task demands (rest vs n-
231 back) in healthy subjects, which was estimated to lie between 6 and 7 percentage points
232 (Cornblath et al., 2020), this value ~~represent~~represented a plausible choice for the small-
233 est effect size of theoretical and practical interest. It also equals the ~~effect size estimated~~
234 estimated effect size based on the data presented in (Schlemm et al., 2022).

235 ~~We used simple bootstrapping~~ Simple bootstrapping was used to create 10 000 hypo-
236 thetical datasets of size 200, 400, 600, 800, 900, 910, ..., 1090, 1100, 1200, 1400, 1500, and
237 1600. Each dataset was then subjected to the estimation procedure described above. For
238 each sample size, the proportion of datasets in which the primary null hypothesis of no
239 association between fractional occupancy and WMH load could be rejected at $\alpha = 0.05$
240 was computed and ~~is~~-recorded as a power curve in Figure 1.

241 ~~It is seen that a~~A sample size of 960 would ~~allow~~have allowed the replication of the
242 reported effect with a power of 80.2 %. We ~~anticipate~~had anticipated a sample size of
243 1500, which ~~yields~~would have yielded a power of 93.9 %.

244 Multiverse analysis

245 ~~Both~~In both (Schlemm et al., 2022) and ~~for~~ our primary replication analysis, we made
246 certain analytical choices in the ~~operationalisation~~operationalization of brain states and

~~247~~ ischemic white matter disease, namely the use of the *36p* confound regression strat-
~~248~~ egy, the Schaefer-400 parcellation, and a BIANCA/LOCATE-based WMH segmentation al-
~~249~~ gorithm. The robustness of the association between WMH burden and time spent in
~~250~~ high-occupancy states with regard to other choices ~~will be was~~ explored in a multiverse
~~251~~ analysis (Steegen et al., 2016). Specifically, in an exploratory analysis, we ~~will estimate~~
~~252~~ ~~estimated~~ brain states from BOLD time series processed according to a variety of estab-
~~253~~ lished confound regression strategies and aggregated over different cortical brain par-
~~254~~ cellations (Table 4, Ceric, Rosen, et al., 2018; Ceric, Wolf, et al., 2017). ~~Extent of cSVD will~~
~~255~~ ~~additionally be~~ ~~The extent of cSVD was additionally~~ quantified by the volume of deep and
~~256~~ periventricular white matter hyperintensities.

~~257~~ For each combination of analytical choice of confound regression strategy, parcella-
~~258~~ tion, and subdivision of white matter lesion load ($9 \times 9 \times 3 = 243$ scenarios in total) ~~we~~
~~259~~ ~~will quantify~~, ~~we quantified~~ the association between WMH load and average time spent
~~260~~ in high-occupancy brain states using odds ~~ratio ratios~~ and 95 % confidence intervals as
~~261~~ described above.

~~262~~ No hypothesis testing ~~and will be carried out in~~ ~~was performed for~~ these multiverse
~~263~~ analyses. ~~They rather~~ ~~Rather, they~~ serve to inform about the robustness of the outcome
~~264~~ of the test of the primary hypothesis. Any substantial conclusions about the association
~~265~~ between ~~the~~ severity of cerebral small ~~pathology and vessel pathology and the~~ time spent
~~266~~ in high-occupancy brain states, ~~as stated in the Scientific Question in Table 3, will be were~~
~~267~~ drawn from the primary analysis using pre-specified methodological choices, ~~as stated~~
~~268~~ ~~in the Scientific Question in Table 3.~~

~~269~~ **Further exploratory analysis**

~~270~~ **Further exploratory analysis**

~~271~~ In previous work, two high-occupancy brain states ~~were have been~~ related to the ~~default-mode~~
~~272~~ ~~default mode~~ network (Cornblath et al., 2020). We ~~will further explore this relation further~~
~~273~~ ~~explored this relationship~~ by computing, for each individual brain state, the cosine simi-
~~274~~ larity of the positive and negative activations of the cluster's centroid with a set of ~~a-priori~~
~~275~~ ~~a priori~~ defined functional 'communities' or networks (Schaefer et al., 2018; Yeo et al.,
~~276~~ 2011). ~~Results will be thus~~ ~~The results were~~ visualized as spider plots for the Schaefer,
~~277~~ Gorden and Power atlases~~atlases~~.

~~278~~ In further exploratory analyses ~~we plan to~~, ~~we~~ describe the associations between

279 brain state dynamics and other measures of cognitive ability, such as memory and lan-
280 guage.

281 **Code and pilot dataResults**

282 Summary data from the first 1000 imaging data points of the HCHS have been published
283 with and form the basis for the hypotheses tested in [For](#) this replication study. We have
284 implemented our prespecified analysis pipeline described above in R and Matlab, and
285 applied it to this previous sample. Data, code and results have been stored on GitHub
286 ([und preserved on Zenodo](#)), a total of 2648 datasets were available, of which 970 were
287 already included in our previous analysis and thus discarded. In 13 of the resulting 1678
288 datasets, one or more MRI sequences were missing. Of the complete datasets (n=1665),
289 we excluded 5 participants due to intra-axial space-occupying lesions. An additional 9
290 subjects were excluded because of unsuccessful preprocessing, WMH segmentation, or
291 xcpEngine failure, resulting in 1651 datasets for analysis. A study-flowchart is provided in
292 [Figure 2](#).

293 Thus re-analysing data from 988 subjects, the separation between two high-occupancy
294 and three

295 Baseline demographic and cognitive values, including the number of missing items,
296 are reported in [Table 6](#).

297 WMH volumes (median 1.05 mL, [IQR](#) 0.47 mL to 2.37 mL), motion estimates, and fractional
298 occupancies of brain states 1 through 5 are reported in [Table 8](#).

299 In an outcome-neutral quality check of the implementation of (i) the MRI processing
300 pipeline, (ii) brain state estimation, and (iii) co-activation pattern analysis, the mean difference
301 in fractional occupancy between high- and low-occupancy [brain states could be reproduced](#)
302 [for all combinations of brain parcellation and confound regression strategies](#) ([??states](#)
303 was significant, with a point-estimate of 6.7 % and a 95 % confidence interval of 6.2 % to
304 7.1 %. This indicates that the implementation of the pipeline was correct and that the
305 brain state estimation and co-activation pattern analysis worked as intended.

306 **Pre-registered hypotheses**

307 Association between WMH load and fractional occupancy

308 The results of the test of our primary preregistered hypothesis of an association between
309 supratentorial WMH volume and the time spent in high-occupancy brain states are shown

310 in Figure 3 and Table 10.

311 Adjusted for age and sex, there was a 0.94-fold reduction in the odds of occupying a
312 high-occupancy brain state for every 5.1-fold increase in WMH load ($P = 5.01 \times 10^{-8}$).

313 **Association between executive function and fractional occupancy in DMN-related
314 states**

315 The results of the test of our secondary preregistered hypothesis of an association between
316 time spent in high-occupancy brain states and executive function as measured by the
317 complete part B of the TMT are shown in Figure 4 and Table 2.

318 **Additional analyses**

319 **Connectivity profiles of brain states – relation to default mode network**

320 Based on the cosine similarity between positive and negative activations of cluster centroids
321 and indicator vectors of pre-defined large scale brain networks, network activation profiles
322 were computed for brain states estimated Schaefer parcellations of varying spatial resolution.

323

324 Figure 6 shows the corresponding spider plots, identifying states characterized by
325 activation (DMN+) or suppression (DMN-) of the default mode network as states with
326 the highest fractional occupancy.

327 **Association with wider cognitive domains**

328 Associations between the time spent in high-occupancy DMN-related brain states and
329 cognitive measures beyond TMT-B are shown in Figure 7.

330 Adjusted for age, sex, WMH load, and years of education, FO appeared to be associated
331 with word recall (aOR 2.4, nominal $P = 0.0153$), but not with global cognitive functioning
332 (MMSE, aOR 1.5), verbal fluency (animal naming, aOR 1.2), vocabulary (aOR 1.5), or pure
333 processing speed (TMT-A, aOR 0.87).

334 **Summary and Discussion**

335 In this pre-registered cross-sectional study we replicated the key findings of Schlemm et al., 2022
336 in an independent population-based sample of 1651 middle-aged to elderly participants
337 of the Hamburg City Health Study.

338 First, we confirmed that the severity of cerebral small vessel disease is associated with
339 the time spent in high-occupancy brain states, defined by functional MRI. More precisely,

340 we showed that every 5.1-fold increase in the volume of supratentorial white matter
341 hyperintensities of presumed vascular origin (WMH) was associated with a 0.95-fold reduction
342 in the odds of occupying a brain state characterized by activation or suppression of the
343 default-mode network, at any given time during the resting-state scan.

344 Second, we confirmed that the time spent in high-occupancy brain states at rest is
345 associated with cognitive performance. More precisely, a 5%-reduction in the fractional
346 occupancy of DMN-related brain states was associated with a 1.02-fold increase in the
347 time to complete part B of the trail making test (TMT).

348 In a pre-planned multiverse analysis, these findings were robust with respect to variations
349 in brain parcellations and confound regression strategies. Inconsistent results were only
350 found with the Desikan–Killiany parcellation irrespective of the confound regression strategy,
351 likely reflecting that the spatial resolution and functional specificity of this coarse, structurally
352 defined atlas are inadequate for analyzing functionally defined brain states.

353 We also confirmed across several brain parcellation resolutions that high-occupancy
354 states at rest are characterized by either activation or suppression of the default mode
355 network, reflecting its role as the predominant task-negative brain network.

356 In unplanned, exploratory analyses, we described the association between brain state
357 dynamics and cognitive measures other than executive function and processing speed
358 and reported a strong, preliminary association between time spent in high-occupancy
359 states and delayed word recall.

360 We further explored, but did not report in detail, the effect of motion; all reported
361 associations were robust to additional, unplanned adjustments for DVARS, RMSD or mean
362 framewise displacement.

363 The presented results provide robust evidence for a behaviorally relevant association
364 between cerebral small vessel disease and functional brain network dedifferentiation.

365 Further research is required to replicate our findings in different populations, such
366 as those affected more severely by cSVD or cognitive impairment, or being studied using
367 different imaging protocols, to determine the generalizability of our findings with respect
368 to varying operationalizations of the notions of cSVD, brain state, and cognition, and to
369 understand the mechanisms underlying the reported associations.

370 **Timeline and access to data**

371 At the time of planning of this study, all demographic, clinical and imaging data used in
372 this analysis ~~have had~~ been collected by the HCHS and ~~are were~~ held in the central trial

³⁷³ database. Quality checks for non-imaging variables ~~have had~~ been performed centrally.
³⁷⁴ WMH segmentation based on structural MRI data of the first 10 000 participants of the
³⁷⁵ HCHS ~~has had~~ been performed previously using the BIANCA/LOCATE approach (Rimmele
³⁷⁶ et al., 2022)~~and results are included in this preregistration (./derivatives/WMH/cSVD_all.csv).~~
³⁷⁷ Functional MRI data and clinical measures of executive dysfunction (TMT-B scores) ~~have~~
³⁷⁸ ~~not had not previously~~ been analyzed by the ~~author. Analysis of the data will begin~~
³⁷⁹ ~~immediately after acceptance in principle of the stage 1 submission of the registered~~
³⁸⁰ ~~report is obtained. Submission of the full manuscript (stage 2) is planned two months~~
³⁸¹ ~~later~~pre-registering author (ES).

³⁸² Acknowledgment

³⁸³ This preprint was created using the LaPreprint template (<https://github.com/roaldarbol/lapreprint>) by Mikkel Roald-Arbøl .

³⁸⁵ References

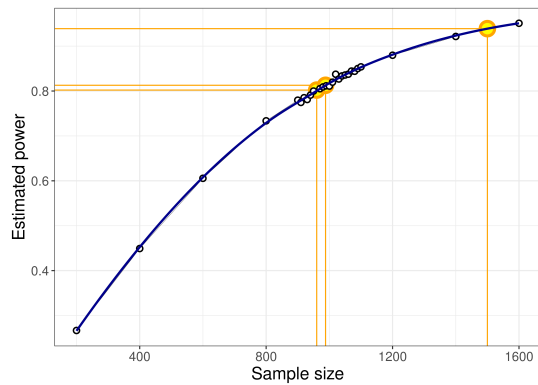
- ³⁸⁶ Arbuthnott, Katherine and Janis Frank (2000). "Trail making test, part B as a measure of
³⁸⁷ executive control: validation using a set-switching paradigm". In: *Journal of clinical and*
³⁸⁸ *experimental neuropsychology* 22.4, pp. 518–528.
- ³⁸⁹ Behzadi, Yashar et al. (2007). "A component based noise correction method (CompCor)
³⁹⁰ for BOLD and perfusion based fMRI". In: *Neuroimage* 37.1, pp. 90–101.
- ³⁹¹ Bos, Daniel et al. (2018). "Cerebral small vessel disease and the risk of dementia: A sys-
³⁹² tematic review and meta-analysis of population-based evidence". en. In: *Alzheimers.*
³⁹³ *Dement.* 14.11, pp. 1482–1492.
- ³⁹⁴ Cannistraro, Rocco J et al. (2019). "CNS small vessel disease: A clinical review". en. In: *Neu-*
³⁹⁵ *rology* 92.24, pp. 1146–1156.
- ³⁹⁶ Ceric, Rastko, Adon FG Rosen, et al. (2018). "Mitigating head motion artifact in functional
³⁹⁷ connectivity MRI". In: *Nature protocols* 13.12, pp. 2801–2826.
- ³⁹⁸ Ceric, Rastko, Daniel H Wolf, et al. (2017). "Benchmarking of participant-level confound
³⁹⁹ regression strategies for the control of motion artifact in studies of functional con-
⁴⁰⁰ nectivity". en. In: *Neuroimage* 154, pp. 174–187.
- ⁴⁰¹ Cornblath, Eli J et al. (2020). "Temporal sequences of brain activity at rest are constrained
⁴⁰² by white matter structure and modulated by cognitive demands". en. In: *Commun Biol*
⁴⁰³ 3.1, p. 261.

- 404 Cox, Robert W (1996). "AFNI: software for analysis and visualization of functional mag-
405 netic resonance neuroimages". In: *Computers and Biomedical research* 29.3, pp. 162–
406 173.
- 407 Das, Alvin S et al. (2019). "Asymptomatic Cerebral Small Vessel Disease: Insights from
408 Population-Based Studies". en. In: *J. Stroke Cerebrovasc. Dis.* 21.2, pp. 121–138.
- 409 Desikan, Rahul S et al. (2006). "An automated labeling system for subdividing the human
410 cerebral cortex on MRI scans into gyral based regions of interest". In: *Neuroimage* 31.3,
411 pp. 968–980.
- 412 Dey, Ayan K et al. (2016). "Pathoconnectomics of cognitive impairment in small vessel
413 disease: A systematic review". en. In: *Alzheimers. Dement.* 12.7, pp. 831–845.
- 414 Esteban, Oscar et al. (2019). "fMRIPrep: a robust preprocessing pipeline for functional
415 MRI". en. In: *Nat. Methods* 16.1, pp. 111–116.
- 416 Frey, Benedikt M et al. (2021). "White matter integrity and structural brain network topol-
417 ogy in cerebral small vessel disease: The Hamburg city health study". en. In: *Hum. Brain
418 Mapp.* 42.5, pp. 1406–1415.
- 419 Friston, Karl J et al. (1996). "Movement-related effects in fMRI time-series". In: *Magnetic
420 resonance in medicine* 35.3, pp. 346–355.
- 421 Gesierich, Benno et al. (2020). "Alterations and test-retest reliability of functional connec-
422 tivity network measures in cerebral small vessel disease". en. In: *Hum. Brain Mapp.*
423 41.10, pp. 2629–2641.
- 424 Glasser, Matthew F et al. (2016). "A multi-modal parcellation of human cerebral cortex".
425 en. In: *Nature* 536.7615, pp. 171–178.
- 426 Gordon, Evan M et al. (2016). "Generation and Evaluation of a Cortical Area Parcellation
427 from Resting-State Correlations". en. In: *Cereb. Cortex* 26.1, pp. 288–303.
- 428 Griffanti, Ludovica, Mark Jenkinson, et al. (2018). "Classification and characterization of
429 periventricular and deep white matter hyperintensities on MRI: A study in older adults".
430 en. In: *Neuroimage* 170, pp. 174–181.
- 431 Griffanti, Ludovica, Giovanna Zamboni, et al. (2016). "BIANCA (Brain Intensity AbNormal-
432 ity Classification Algorithm): A new tool for automated segmentation of white matter
433 hyperintensities". en. In: *Neuroimage* 141, pp. 191–205.
- 434 Jagodzinski, Annika et al. (2020). "Rationale and Design of the Hamburg City Health Study".
435 en. In: *Eur. J. Epidemiol.* 35.2, pp. 169–181.

- ⁴³⁶ Laumann, Timothy O, Evan M Gordon, et al. (2015). "Functional system and areal organization of a highly sampled individual human brain". In: *Neuron* 87.3, pp. 657–670.
- ⁴³⁷
- ⁴³⁸ Laumann, Timothy O and Abraham Z Snyder (2021). "Brain activity is not only for thinking". In: *Current Opinion in Behavioral Sciences* 40, pp. 130–136.
- ⁴³⁹
- ⁴⁴⁰ Laumann, Timothy O, Abraham Z Snyder, et al. (2017). "On the stability of BOLD fMRI correlations". In: *Cerebral cortex* 27.10, pp. 4719–4732.
- ⁴⁴¹
- ⁴⁴² Lawrence, Andrew J, Ai Wern Chung, et al. (2014). "Structural network efficiency is associated with cognitive impairment in small-vessel disease". en. In: *Neurology* 83.4, pp. 304–311.
- ⁴⁴³
- ⁴⁴⁴
- ⁴⁴⁵ Lawrence, Andrew J, Daniel J Tozer, et al. (2018). "A comparison of functional and tractography based networks in cerebral small vessel disease". en. In: *Neuroimage Clin* 18, pp. 425–432.
- ⁴⁴⁶
- ⁴⁴⁷
- ⁴⁴⁸ Lawrence, Andrew J, Eva A Zeestraten, et al. (2018). "Longitudinal decline in structural networks predicts dementia in cerebral small vessel disease". en. In: *Neurology* 90.21, e1898–e1910.
- ⁴⁴⁹
- ⁴⁵⁰
- ⁴⁵¹ Macey, Paul M et al. (2004). "A method for removal of global effects from fMRI time series". In: *Neuroimage* 22.1, pp. 360–366.
- ⁴⁵²
- ⁴⁵³ Makris, Nikos et al. (2006). "Decreased volume of left and total anterior insular lobule in schizophrenia". In: *Schizophrenia research* 83.2-3, pp. 155–171.
- ⁴⁵⁴
- ⁴⁵⁵ Muschelli, John et al. (2014). "Reduction of motion-related artifacts in resting state fMRI using aCompCor". In: *Neuroimage* 96, pp. 22–35.
- ⁴⁵⁶
- ⁴⁵⁷ Petersen, Marvin et al. (2020). "Network Localisation of White Matter Damage in Cerebral Small Vessel Disease". en. In: *Sci. Rep.* 10.1, p. 9210.
- ⁴⁵⁸
- ⁴⁵⁹ Power, Jonathan D, Alexander L Cohen, et al. (2011). "Functional network organization of the human brain". en. In: *Neuron* 72.4, pp. 665–678.
- ⁴⁶⁰
- ⁴⁶¹ Power, Jonathan D, Anish Mitra, et al. (2014). "Methods to detect, characterize, and remove motion artifact in resting state fMRI". In: *Neuroimage* 84, pp. 320–341.
- ⁴⁶²
- ⁴⁶³ Prins, Niels D et al. (2005). "Cerebral small-vessel disease and decline in information processing speed, executive function and memory". en. In: *Brain* 128.Pt 9, pp. 2034–2041.
- ⁴⁶⁴
- ⁴⁶⁵ Pruim, Raimon HR et al. (2015). "ICA-AROMA: A robust ICA-based strategy for removing motion artifacts from fMRI data". In: *Neuroimage* 112, pp. 267–277.
- ⁴⁶⁶
- ⁴⁶⁷ Reijmer, Yael D et al. (2016). "Small vessel disease and cognitive impairment: The relevance of central network connections". en. In: *Hum. Brain Mapp.* 37.7, pp. 2446–2454.
- ⁴⁶⁸

- ⁴⁶⁹ Rimmele, David Leander et al. (2022). "Association of Carotid Plaque and Flow Velocity
⁴⁷⁰ With White Matter Integrity in a Middle-aged to Elderly Population". en. In: *Neurology*.
⁴⁷¹ Satterthwaite, Theodore D et al. (2013). "An improved framework for confound regres-
⁴⁷² sion and filtering for control of motion artifact in the preprocessing of resting-state
⁴⁷³ functional connectivity data". In: *Neuroimage* 64, pp. 240–256.
- ⁴⁷⁴ Schaefer, Alexander et al. (2018). "Local-Global Parcellation of the Human Cerebral Cortex
⁴⁷⁵ from Intrinsic Functional Connectivity MRI". en. In: *Cereb. Cortex* 28.9, pp. 3095–3114.
- ⁴⁷⁶ Schlemm, Eckhard et al. (2022). "Equalization of Brain State Occupancy Accompanies
⁴⁷⁷ Cognitive Impairment in Cerebral Small Vessel Disease". en. In: *Biol. Psychiatry* 92.7,
⁴⁷⁸ pp. 592–602.
- ⁴⁷⁹ Schulz, Maximilian et al. (2021). "Functional connectivity changes in cerebral small vessel
⁴⁸⁰ disease - a systematic review of the resting-state MRI literature". en. In: *BMC Med.* 19.1,
⁴⁸¹ p. 103.
- ⁴⁸² Shen, Jun et al. (2020). "Network Efficiency Mediates the Relationship Between Vascular
⁴⁸³ Burden and Cognitive Impairment: A Diffusion Tensor Imaging Study in UK Biobank".
⁴⁸⁴ en. In: *Stroke* 51.6, pp. 1682–1689.
- ⁴⁸⁵ Steegen, Sara et al. (2016). "Increasing Transparency Through a Multiverse Analysis". en.
⁴⁸⁶ In: *Perspect. Psychol. Sci.* 11.5, pp. 702–712.
- ⁴⁸⁷ Sundaresan, Vaanathi et al. (2019). "Automated lesion segmentation with BIANCA: Im-
⁴⁸⁸ pact of population-level features, classification algorithm and locally adaptive thresh-
⁴⁸⁹ olding". en. In: *Neuroimage* 202, p. 116056.
- ⁴⁹⁰ Tombaugh, Tom N (2004). "Trail Making Test A and B: normative data stratified by age
⁴⁹¹ and education". en. In: *Arch. Clin. Neuropsychol.* 19.2, pp. 203–214.
- ⁴⁹² Tuladhar, Anil M, Ewoud van Dijk, et al. (2016). "Structural network connectivity and cog-
⁴⁹³ nition in cerebral small vessel disease". en. In: *Hum. Brain Mapp.* 37.1, pp. 300–310.
- ⁴⁹⁴ Tuladhar, Anil M, Jonathan Tay, et al. (2020). "Structural network changes in cerebral small
⁴⁹⁵ vessel disease". en. In: *J. Neurol. Neurosurg. Psychiatry* 91.2, pp. 196–203.
- ⁴⁹⁶ Tzourio-Mazoyer, Nathalie et al. (2002). "Automated anatomical labeling of activations in
⁴⁹⁷ SPM using a macroscopic anatomical parcellation of the MNI MRI single-subject brain".
⁴⁹⁸ In: *Neuroimage* 15.1, pp. 273–289.
- ⁴⁹⁹ Vidaurre, Diego et al. (2018). "Discovering dynamic brain networks from big data in rest
⁵⁰⁰ and task". en. In: *Neuroimage* 180.Pt B, pp. 646–656.

- 501 Wardlaw, Joanna M, Colin Smith, and Martin Dichgans (2013). "Mechanisms of sporadic
502 cerebral small vessel disease: insights from neuroimaging". en. In: *Lancet Neurol.* 12.5,
503 pp. 483–497.
- 504 Wardlaw, Joanna M, Eric E Smith, et al. (2013). "Neuroimaging standards for research
505 into small vessel disease and its contribution to ageing and neurodegeneration". en.
506 In: *Lancet Neurol.* 12.8, pp. 822–838.
- 507 Wardlaw, Joanna M, María C Valdés Hernández, and Susana Muñoz-Maniega (2015). "What
508 are white matter hyperintensities made of? Relevance to vascular cognitive impair-
509 ment". en. In: *J. Am. Heart Assoc.* 4.6, p. 001140.
- 510 Xu, Yuanhang et al. (2021). "Altered Dynamic Functional Connectivity in Subcortical Is-
511 chemic Vascular Disease With Cognitive Impairment". en. In: *Front. Aging Neurosci.* 13,
512 p. 758137.
- 513 Yeo, B T Thomas et al. (2011). "The organization of the human cerebral cortex estimated
514 by intrinsic functional connectivity". en. In: *J. Neurophysiol.* 106.3, pp. 1125–1165.
- 515 Yin, Wenwen et al. (2022). "The Clustering Analysis of Time Properties in Patients With
516 Cerebral Small Vessel Disease: A Dynamic Connectivity Study". en. In: *Front. Neurol.*
517 13, p. 913241.



Estimated power for different sample sizes is obtained as the proportion of synthetic data sets in which the null hypothesis of no association between WMH volume and time spent in high-occupancy brain states can be rejected at the $\alpha = 0.05$ significance level. Proportions are based on a total of 10 000 synthetic data sets obtained by bootstrapping the data presented in . Highlighted in orange are the smallest sample size ensuring a power of at least (n = 960), the sample size of the pilot data (n = 988, post-hoc power), and the expected sample size for this replication study (n = 1500, a-priori power).

Figure 1 | Sample size and power estimation. A-priori estimated power for different sample sizes was obtained as the proportion of synthetic data sets in which the null hypothesis of no association between WMH volume and time spent in high-occupancy brain states can be rejected at the $\alpha = 0.05$ significance level. Proportions are based on a total of 10 000 synthetic data sets obtained by bootstrapping the data presented in (Schlemm et al., 2022). Highlighted in orange are the smallest sample size ensuring a power of at least 80 % (n = 960), the sample size of the pilot data (n = 988, post-hoc power 81.3 %), and the expected sample size for this replication study (n = 1500, a-priori power 93.9 %).

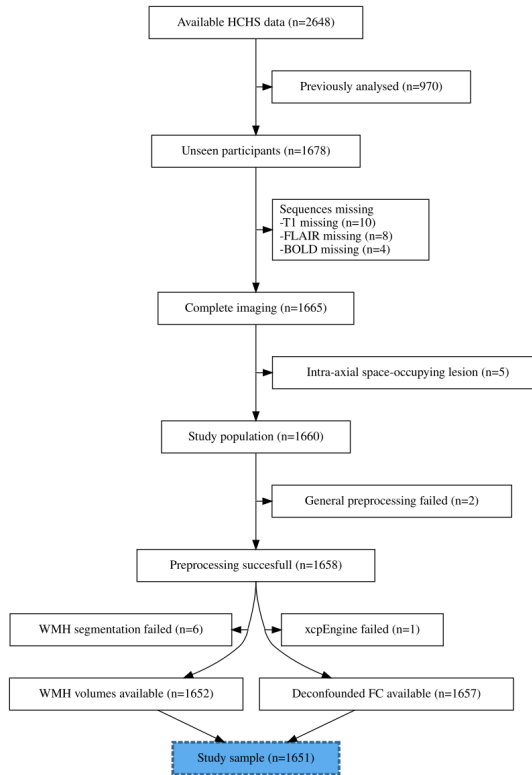


Figure 2 | Study flowchart. Composition of the study population after application of inclusion and exclusion criteria, and image processing.

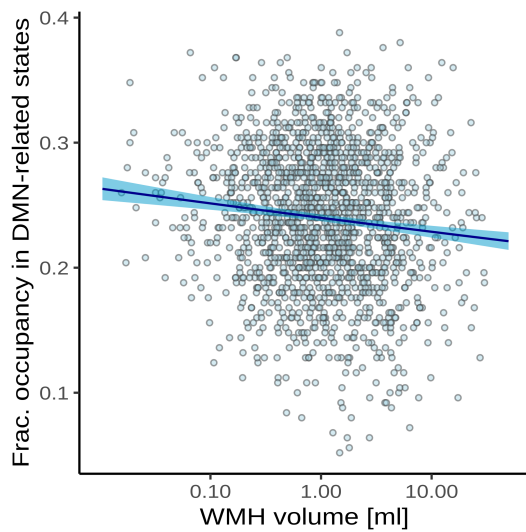


Figure 3 | Association between time spent in high-occupancy brain states and supratentorial WMH volume. Point estimates (black line) and 95%-confidence region (light blue ribbon) of the conditional mean fractional occupancy are obtained from unadjusted beta regression modelling. Each marker represents one of N=1642 independent subjects with a non-zero total WMH volume.

Point estimates (dots) and confidence intervals (line segments) for the mean difference in fractional occupancy between high- and low-occupancy states are shown for different confound regression strategies (groups along the vertical axis) and brain parcellations (color). The difference in FO for a particular choice of regression strategy and brain parcellation is nominally statistically significantly different from zero at a significance level of 5% if the corresponding interval does not contain zero. Hence, the FO difference is significant for *all* processing choices, reflecting the separation between high- and low-occupancy states. The primary choices (36p and schaefer400) are highlighted by a yellow box and thick pink line, respectively. The effect size reported in is indicated by a

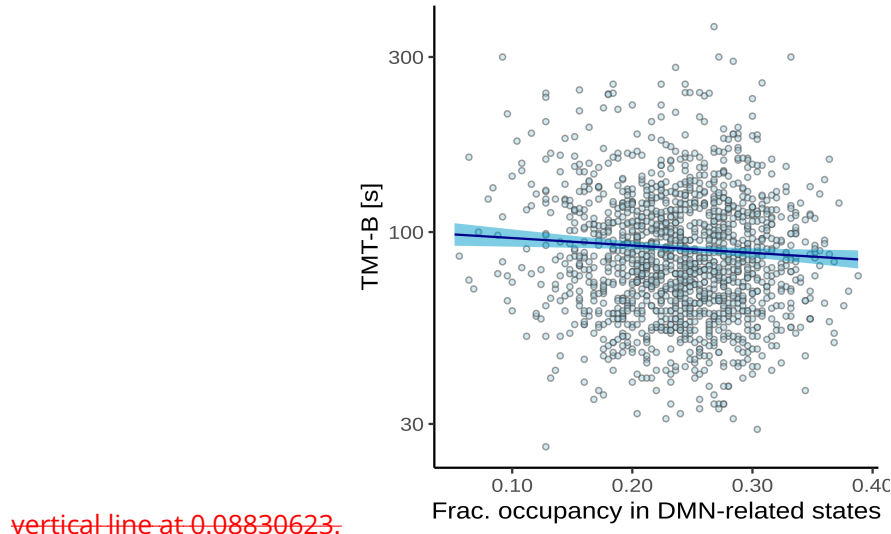


Figure 4 | Association between time spent in high-occupancy DMN-related brain states and TMT-B completion time. Point estimates (black line) and 95%-confidence region (light blue ribbon) of the conditional mean TMT-B completion time are obtained from unadjusted Gamma regression modelling. Each marker represent one of N=1482 independent subjects with non-zero total WMH volume and available TMT-B data.

	Estimate	P	95%-CI
Intercept	53.41	< 0.0001	42.7 – 66.8
FO.high, per 5%	0.98	0.0116	0.96 – 0.99
log WMH [†] , per 5.1-fold increase ¹	1.01	0.367	0.98 – 1.05
Age, per 10 years	1.18	< 0.0001	1.15 – 1.21
Female sex	0.99	0.666	0.95 – 1.03
Education, per year	0.97	< 0.0001	0.97 – 0.98
$\mathbf{1}_{\{\text{WMH}=0\}}$	0.97	0.398	0.92 – 1.03

¹ Interquartile ratio $2.37/0.468 = 5.06$

Table 2 | Association between TMT-B and time spent in high-occupancy DMN-related brain states adjusted for age, sex, WMH volume and years of education. Gamma regression table estimated from $n = 1483$ independent participants using the model equation

$$\text{TMT-B} \sim \text{FO}^{\text{high}} + \log \text{WMH}^+ + \mathbf{1}_{\{\text{WMH}=0\}} + \text{age} + \text{sex}$$

~

518 Adjusted for age, sex, WMH volume, and years of education, there was a 0.98-fold
 519 reduction in the time to complete the TMT-B for every 5 % increase in the time spent in
 520 high-occupancy brain states ($P = 0.0116$).

521 Multiverse analysis

522 In a multiverse analysis, the main finding was somewhat robust with respect to the choices of brain parcellation and confound regression strategy.
 523 WMH load and FO and between FO and TMT-B were robust with respect to these choices.
 524 The processing choices of brain parcellation and confound regression strategy.
 525 A nominally statistically significant negative association between the total WMH load and time spent in high-occupancy states was observed in 1948/81 scenarios, with 59/81

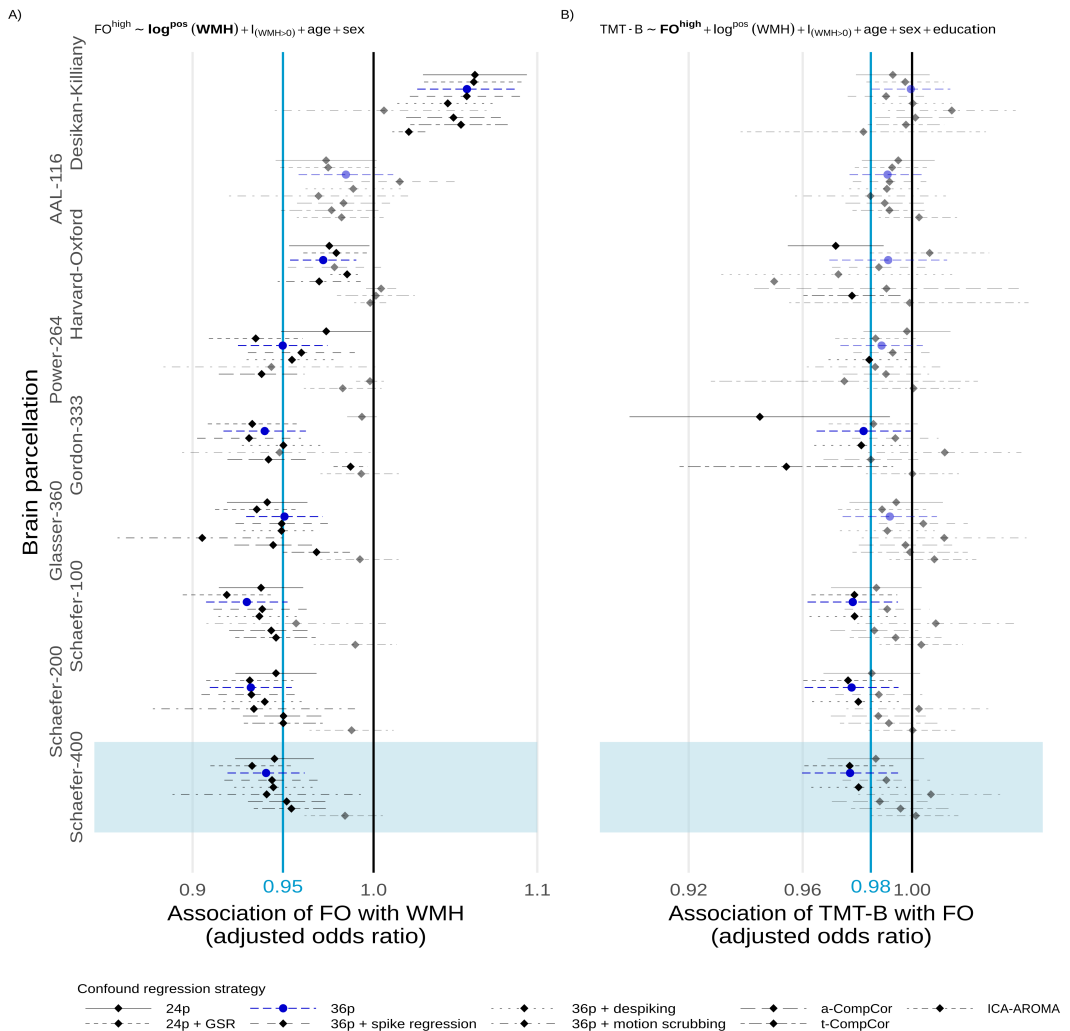


Figure 5 | Multiverse analysis. Adjusted effect size estimates of the associations between cSVD severity (WMH volume) and network dedifferentiation (less time spent in high-occupancy DMN-related brain states) [A]), and between network dedifferentiation and executive function (TMT-B completion time) [B]). Effect sizes are given per 5.1-fold increase in WMH volume and a 5%-increase in fractional occupancy, respectively. Markers and line segments indicate point estimates and 95%-confidence intervals for adjusted odds ratios for different combinations of confound regression strategy and brain parcellation. The primary analytical choices are indicated by dark blue circles (36p) and light blue shading (Schaefer-400). Model equations for beta and gamma regressions, respectively, are given at the top. Vertical lines indicate no effect (black) and the effect size observed in the discovery cohort (Schlemm et al., 2022) (light blue), respectively, for reference. Effect sizes not reaching nominal statistical significance ($\alpha = 0.05$) are shown desaturated. Corresponding data based on periventricular and deep WMH volumes are given in the Supplement.

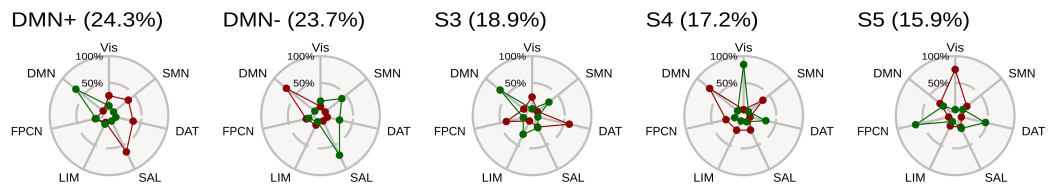


Figure 6 | Connectivity profiles of brain states. Cosine similarity between centroids of each identified brain state and signed indicator vectors corresponding to activation (green) and suppression (red) of each of seven predefined large-scale functional brain networks (Yeo et al., 2011). Parenthetical percentages indicate the mean fractional occupancy across N=1651 independent subjects. Two high-occupancy states are characterized by activation or suppression of the DMN, the remaining three low-occupancy states (S3–5) were not used in the present study.

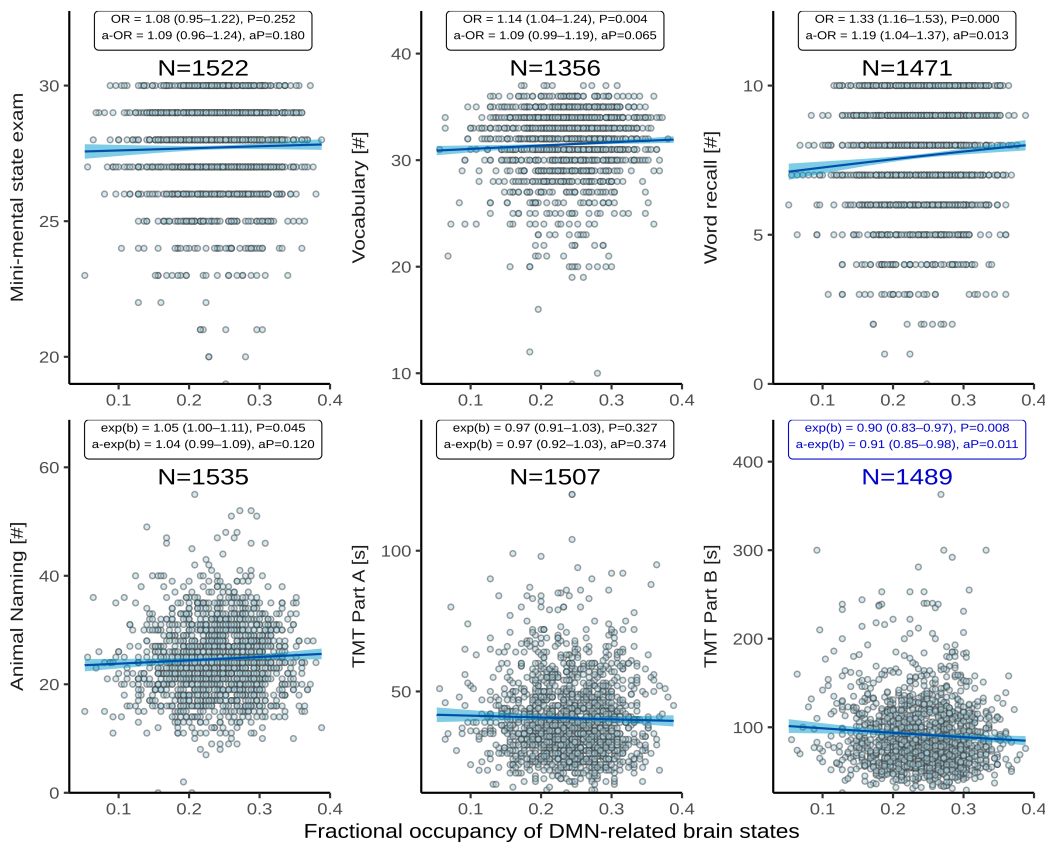


Figure 7 | Association between time spent in high-occupancy DMN-related brain states and cognitive measures. Point estimates (black line) and 95%-confidence region (light blue ribbon) of the conditional mean cognitive measures are obtained from unadjusted binomial (top row: Mini-Mental State Examination, Vocabulary, Word List Recall, logit link) and Gamma regression (bottom row: Animal Naming, Trail Making Test [TMT] A/B: log link) modelling. Each marker represents one of N independent subjects, as indicated. Insets report effect sizes and P-values both with (adjusted [a-]) and without adjustment for the nuisance variables age, sex, WMH volume (coded as in Figure 5), and years of education. Effect sizes were quantified as odds ratios (ORs) (top) or response scale multipliers [exp(b)] (bottom), and correspond to a 20%-increase in fractional occupancy. Note the different reference change in FO compared to Table 2 chosen to adequately represent some of the smaller effect sizes. The bottom right panel highlighted in dark blue reproduces Figure 4.

Question	Hypothesis	Sampling plan	Analysis plan	Rationale for deciding the sensitivity of the test	Interpretation given different outcomes	Theory that could be shown wrong by the outcome
Is severity of cerebral small disease, quantified by the volume of supratentorial white matter hyperintensities of presumed vascular origin (WMH), associated with time spent in high-occupancy brain states, defined by resting-state functional MRI?	(Primary) Higher WMH volume is associated with lower average occupancy of the two highest-occupancy brain states. (Secondary) Lower average occupancy of the two highest-occupancy brain states is associated with longer TMT-B time.	Available subjects with clinical and imaging data from the HCHS (Jagodzinski et al., 2020)	Standardized preprocessing of structural and functional MRI data • automatic quantification of WMH • co-activation pattern analysis • multivariable generalised regression analyses	Tradition	$P < 0.05 \rightarrow$ rejection of the null hypothesis of no association between cSVD and fractional occupancy; $P > 0.05 \rightarrow$ insufficient evidence to reject the null hypothesis	Functional brain dynamics are not related to subcortical ischemic vascular disease.
Is time spent in high-occupancy brain states associated with cognitive impairment, measured as the time to complete part B of the trail making test (TMT)?	as above	as above	as above	as above	$P < 0.05 \rightarrow$ rejection of the null hypothesis of no association between fractional occupancy and cognitive impairment; $P > 0.05 \rightarrow$ insufficient evidence to reject the null hypothesis	Cognitive function is not related to MRI-derived functional brain dynamics.

Study Design Template

Table 3 | Study Design Template. Overview of the Scientific Questions addressed in the present study (first column), the two main hypotheses being investigated (second column), and details of the underlying study.

Name of the atlas	#parcels	Reference	Design	Reference
Desikan-Killiany	86	Desikan et al., 2006	24p	Friston et al., 1996
AAL	116	Tzourio-Mazoyer et al., 2002	24p + GSR	Macey et al., 2004
Harvard-Oxford	112	Makris et al., 2006	36p	Satterthwaite et al., 2013
glasser360	360	Glasser et al., 2016	36p + spike regression	Cox, 1996
gordon333	333	Gordon et al., 2016	36p + despiking	Satterthwaite et al., 2013
power264	264	Power, Cohen, et al., 2011	36p + scrubbing	Power, Mitra, et al., 2014
schaefer{N}	100	Schaefer et al., 2018	aCompCor	Muschelli et al., 2014
	200		tCompCor	Behzadi et al., 2007
	400		AROMA	Pruim et al., 2015

AAL: Automatic Anatomical Labelling

(a) Parcellations

GSR: Global signal regression, AROMA: Automatic Removal of Motion Artifacts

(b) Confound regression strategies, adapted from (Ciric, Wolf, et al., 2017)

Multiverse analysis, implemented using xcpEngine

Table 4 | Multiverse analysis. Overview over different brain parcellations and confound regression strategies implemented using xcpEngine (Ciric, Rosen, et al., 2018). A total of $9 \times 9 = 81$ analytical combinations were explored to assess the robustness of our results with respect to these processing choices.

N = 1,651	
<i>Demographics (no Missing n (%))</i>	
Age	
Median (IQR)	66 (59 - 72)
Sex	
Male	940/1651 (57%)
Female	711/1651 (43%)
<i>Cardiovascular risk factors</i>	
Hypertension	
Present	1177/1611 (73.1%)
Missing n (%)	85 (5.1%)
Diabetes	
Present	157/1566 (10%)
Missing n (%)	40 (2.4%)
Smoking	
Present	200/1360 (14.7%)
Missing n (%)	201 (12.9%)
Hyperlipidaemia	
Present	426/1578 (27%)
Missing n (%)	73 (4.4%)
<i>Cognitive test results</i>	
MMSE (#, max. 30)	
Median (IQR)	28 (27 - 29)
Missing n (%)	129 (7.8%)
Vocabulary (MWT-B) (#, max. 37)	
Median (IQR)	32 (30 - 34)
Missing n (%)	295 (18%)
Word recall #, (max. 10)	
Median (IQR)	8 (6 - 9)
Missing n (%)	180 (11%)
Animal Naming	
Median (IQR)	24 (20 - 29)
Missing n (%)	116 (7.0%)
TMT-A, seconds	
Median (IQR)	38 (31 - 48)
Missing n (%)	144 (8.7%)
TMT-B, seconds	
Median (IQR)	83 (65 - 110)
Missing n (%)	162 (9.8%)
<i>History</i>	
Diagnosed dementia	
Present	6/1645 (0.4%)
Missing n (%)	6 (0.4%)
Years of education	
Median (IQR)	13 (12 - 16)
Missing n (%)	34 (2%)

Table 6 | Descriptive statistics of the study population. Data are presented as median (interquartile range) or count (percentage) of non-missing items, as appropriate. Number of percentage of missing items are reported separately.

N = 1,651	
<u>WMH volume¹, ml</u>	
Total	1.05 (0.47 – 2.37), 9 Z
Periventricular	0.94 (0.43 – 2.04), 9 Z
Deep	0.10 (0.03 – 0.37), 344 Z
<u>Motion during rs-fMRI</u>	
Framewise displacement, mm	0.21 (0.15 – 0.63)
RMSD, mm	0.086 (0.058 – 0.12)
DVARS	27.8 (24.3 – 31.8)
<u>Fractional occupancy, %</u>	
DMN+	24.8 (20.8 – 28.0)
DMN-	24.0 (20.0 – 28.0)
S3	18.4 (15.2 – 22.4)
S4	16.8 (12.8 – 20.8)
S5	15.2 (12.0 – 19.2)

¹Number of zero values indicated by Z

Table 8 | Structural and functional imaging characteristics. Data are presented as median (interquartile range). Supratentorial WMH volumes were obtained by semiautomatic segmentation of FLAIR images using a BINACA/LOCATE-based k -nearest neighbours algorithm and stratified by their distance to the lateral ventricles (<10 mm, periventricular; >10 mm, deep). Motion parameters were estimated during fMRIprep processing of BOLD scans. Fractional occupancies were calculated by assigning individual BOLD volumes to one of five discrete brain states defined by k-means clustering-based co-activation pattern analysis.

	Estimate	P	95%-CI
Intercept	0.24	<0.0001	0.21 – 0.27
$\log \text{WMH}^+$, per 5.1-fold increase ¹	0.94	<0.0001	0.92 – 0.96
Age, per 10 years	1.04	0.001	1.01 – 1.06
Female sex	1.12	<0.0001	1.09 – 1.16
$\mathbf{1}_{\{\text{WMH}=0\}}$	0.93	0.477	0.75 – 1.14

¹ Interquartile ratio $2.37/0.468 = 5.06$

Table 10 | Association between time-spent in high-occupancy DMN-related brain states and WMH adjusted for age and sex. Beta regression table estimated from $n = 1651$ independent participants using the model equation $\text{FO}^{\text{high}} \sim \log \text{WMH}^+ + \mathbf{1}_{\{\text{WMH}=0\}} + \text{age} + \text{sex}$.